2

Conf-911132--20

GA–A20743

RECYCLING AND PARTICLE CONTROL IN DIII–D

by

G.L. JACKSON and the DIII–D TEAM

NOVEMBER 1991

GENERAL ATOMICS

DISCLAIMER

GA-A--20743

DE92 007944

RECYCLING AND PARTICLE CONTROL IN DIII–D

by

G.L. JACKSON and the DIII–D TEAM

This is a preprint of an invited paper to be presented at the 38th Annual American Vacuum Society Symposium and Topical Conference, November 11–15, 1991, Seattle, Washington, and to be printed in the *Proceedings*.

Work supported by
U.S. Department of Energy
Contract DE-AC03-89ER51114

GENERAL ATOMICS PROJECT 3466
NOVEMBER 1991

GENERAL ATOMICS

ABSTRACT

Particle control of both hydrogen and impurity atoms is important in obtaining reproducible discharges with a low fraction of radiated power in the DIII–D tokamak. The main DIII–D plasma facing components are graphite tiles (40% of the total area and covering regions exposed to the highest heat fluxes) and Inconel. Hydrogenic species desorbed from graphite during a tokamak discharge can be a major fueling source, especially in unconditioned graphite where these species can saturate the surface regions. In this case the recycling coefficient can exceed unity, leading to an uncontrolled density rise. In addition to removing volatile hydrocarbons and oxygen, DIII–D vessel conditioning efforts have been directed at the reduction of particle fueling from the graphite tiles. Conditioning techniques include: baking to $\leq$400°C, low power pulsed discharge cleaning, and glow discharges in deuterium, helium, neon, or argon. Helium glow wall conditioning, is now routinely performed before every tokamak discharge. The effects of these techniques on hydrogen recycling and impurity influxes will be presented. The Inconel walls, while not generally exposed to high heat fluxes, nevertheless represent a source of metal impurities which can lead to impurity accumulation in the discharge and a high fraction of radiated power, particularly in H–mode discharges at higher plasma currents, $I_p > 1.5$ MA. To reduce metal influx a thin ($\sim$100 nm) low Z film (carbon or boron) has been applied on all plasma facing surfaces in DIII–D. The application of the boron film, referred to as boronization, has the additional benefit over a carbon film (carbonization) of further reducing the

oxygen influx. Following the first boronization in DIII–D a regime of very high confinement (VH–mode) was observed, characterized by low ohmic target density, low Z_{eff}, and low radiated power.

I. INTRODUCTION

There has been steady progress in the last two decades towards the demonstration of the break-even condition in fusion research. This progress has often been coupled to improved wall materials and better conditioning techniques for impurity control and lower recycling.[1-4] The DIII–D program at General Atomics has made significant contributions to this steady progress, and wall materials and conditioning have played an important role. Some of these conditioning techniques for a dominantly metallic wall are based on work in the Doublet III tokamak. These techniques were discussed in a previous paper.[5] The introduction of graphite as the major high heat flux first wall material in DIII–D significantly reduced metallic impurities, but required implementation of new conditioning techniques to reduce recycling and low Z impurities. Further conditioning using wall coating techniques has recently been applied to further reduce recycling and impurities. The conditioning techniques used on DIII–D are listed in Table I in the chronological order in which they were implemented.

In this paper we will discuss the effectiveness of the various methods employed in DIII–D to reduce impurity contamination of the tokamak plasmas (Section II) and achieve recycling control (Section III). In Section IV we will describe a model of the wall fueling after boronization and present conclusions. We define wall conditioning to include the application of a thin film of carbon or boron to the plasma facing surfaces, called carbonization and boronization respectively.

Table I
Conditioning Techniques in DIII–D

Technique	Main Benefit	When Applied	Typical Parameters	Improvements in Tokamak Discharges
Baking	Impurity removal, desorb H_2 for lower recycling	After machine opening, isotope changeover, low recycling	T $\leq$450°C inside wall, $\leq$350°C outside wall	Used primarily in conjunction with other techniques.
Taylor type pulsed discharge cleaning (TDC)	Oxygen and hydrocarbon removal	After machine opening	$I_p \sim 10$ kA, V_{LOOP} 15 V, P $\sim$ 0.1–0.2 mT (abs) H_2 or D_2	Baseline conditioning technique used extensively through 1987 and after machine openings.
Hydrogen glow discharge cleaning	Impurity removal	After a disruption (followed by HeGWC) or after machine opening	I $\lesssim$ 8 A, V $\sim$ 250–400 V	Enhances recovery after disruptions.
Helium glow wall conditioning (HeGWC)	Hydrogen desorption (lower recycling) and impurity removal	Routinely applied before every tokamak discharge	$T_{wall} \sim$ 20–40°C V_{anode} = 300–500 V $I_{anode} \sim$ 1–7 A, typ. α ($\lesssim$ 8 μA/cm^2) P $\sim$ 1–4 mTorr	After routine application: – Lower recycling and $\bar{n}_e$ (ohmic) – Observation of ohmic H–mode – Observation of limiter H–mode – Faster disruption recovery – Reliable low q operation (leading to higher achievable β_T)
Neon (argon) glow discharge conditioning	Attempt to reduce recycling and control $\bar{n}_e$ during H–mode	Low recycling experiments		Hydrogen recycling is reduced but radiated power from neon (argon) retained in the walls limits its effectiveness.
Carbonization	Reduce metal impurity influx, especially during H–mode discharges	Before high current operation	30–80 nm carbon film applied to all plasma facing surfaces at 150°C then bake to 350°C	Peaked density profiles observed during H–mode. 3 MA double-null discharges obtained and highest values of stored energy to date (3.5 MJ).
Boronization	Reduce oxygen influx and recycling. Also lower metal impurity influx.	Monthly since May 1991 (when tokamak is operating)	100–150 nm boron film applied using a glow discharge 0.9 He, 0.1 B_2D_6 at 250°C to 300°C	First observation of very high confinement mode (VH–mode) and highest triple product $n_D(0)\tau_e T_i(0) = 2\times10^{20}$ m^{-3}-sec-keV. Routine operation at 3 MA was attained. $W \leq$ 3.6 MJ.

II. WALL CONDITIONING FOR IMPURITY CONTROL

The first techniques used in DIII–D to condition the vessel were pulsed (Taylor) discharge cleaning and baking, $T_{av} \leq 400°C$[6] (the vessel appendages are also heated to $\leq 200°C$). These techniques were sufficient to reduce the impurity contamination of tokamak plasmas, allowing the achievement of H–mode with an open single-null divertor configuration.[7] The initial installation of POCO graphite tiles covered 9% of the plasma facing surface, primarily in the lower divertor region.

In order obtain low Z_{eff} plasma discharges at higher currents and auxiliary heating powers, graphite coverage was increased from 9% to 40% in 1988. The floor, ceiling, and inner wall of DIII–D are now all graphite (Union Carbide TS-1792). Baking and TDC again reduced the impurity content of plasma discharges after this vessel opening. During this period, deuterium (or hydrogen) glow discharge cleaning and helium glow wall conditioning (HeGWC) were developed and HeGWC is now routinely applied before every tokamak discharge. Deuterium is used as the fill gas and the neutral beam specie in most DIII–D discharges and in this paper we will refer to deuterium to mean either hydrogenic isotope: hydrogen or deuterium. Both deuterium and helium glow discharges can be used to remove impurities. An example of the dominant impurity gases removed during a combined session of D_2 glow followed by a helium glow discharge is shown in Fig. 1. Masses 30 and 32 are primarily hydrocarbons during the deuterium glow, while masses 18, 20, and 28 contain both oxygen and carbon: CD_3, DO, CD_4, D_2O, C_2D_2, and CO. More than (>90%) of all

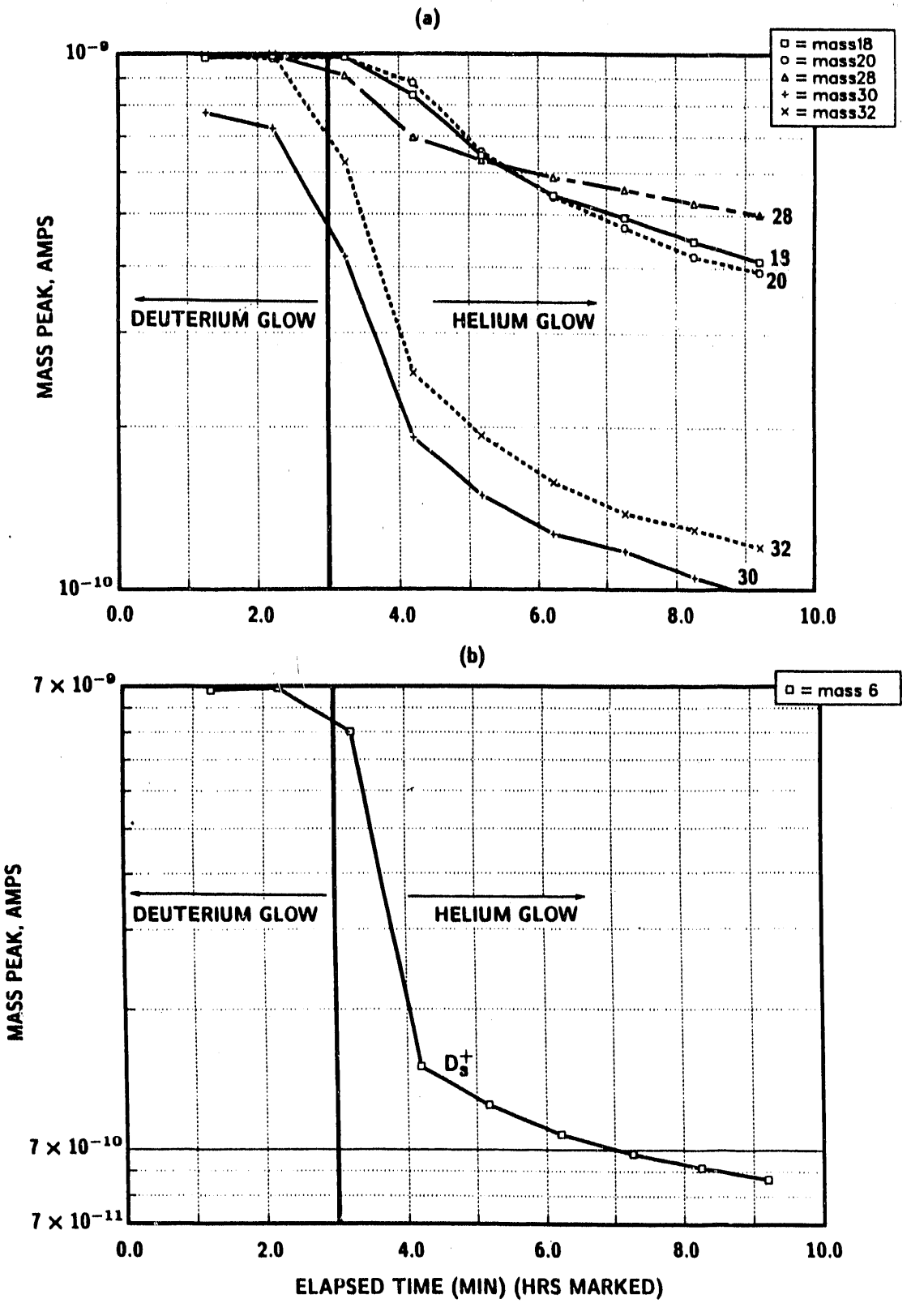

Fig. 1. Residual gas analyzer (RGA) analysis of the the main impurity gases (a) and D_3^+ (b) during a combined session of deuterium glow ($t \leq 3$ min) followed by helium glow. ($\bar{V}_{\text{anode}} = 340$ V, $\bar{I}_{\text{total}} = 4.7$ Amps.) RGA saturation occurs at a partial pressure corresponding to 1×10^{-9} Amps.

tokamak discharges are preceded by HeGWC only (no D_2 glow). However deuterium glow has sometimes been used after a high power disruption (typically $I_p > 2$ MA and $P_{beam} > 10$ MW) to remove any loosely bound carbon or oxygen. Deuterium or hydrogen glow discharges are also employed for isotope changeover, *i.e.* changing from hydrogen to deuterium fill gas or vice versa. As discussed in the next section, a helium glow lowers the particle fueling from the walls, and therefore it follows a deuterium glow discharge, as shown in Fig. 1.

The techniques described above are effective in removing oxygen and loosely bound carbon, and produced operation up to 2.5 MA and 20 MW of neutral beam power. However, during the quiescent phase of some higher current H–mode discharges ($I_p > 1.5$ MA), radiated power and high Z metal impurities accumulated in the discharge. Under some conditions, the radiated power could equal the auxiliary heating power and a radiation collapse of the discharge could occur. The source of these metal impurities was the Inconel outer wall which comprises 60% of the plasma facing surface. Significant metal impurities were observed even though the Inconel surfaces were not directly exposed to known areas of high heat flux. To reduce this metal influx a thin hard low Z coating can be applied to the Inconel walls. Carbonization consists of applying a carbon film ~100 nm thick with glow discharge of helium and methane to cover the metal surfaces. It was implemented in DIII–D and successfully reduced the influx of metal impurities and lowered the radiated power, as shown in Fig. 2. After carbonization, the first 3 MA discharges in DIII–D were obtained and low q, high β_T discharges, (up to 11%) were also achieved.[9]

Although carbonization successfully reduced high Z impurities, and to a lesser degree oxygen, low Z impurities could still produce a high fraction of radiated power at high plasma currents. Based on the results from the TEXTOR device, a system

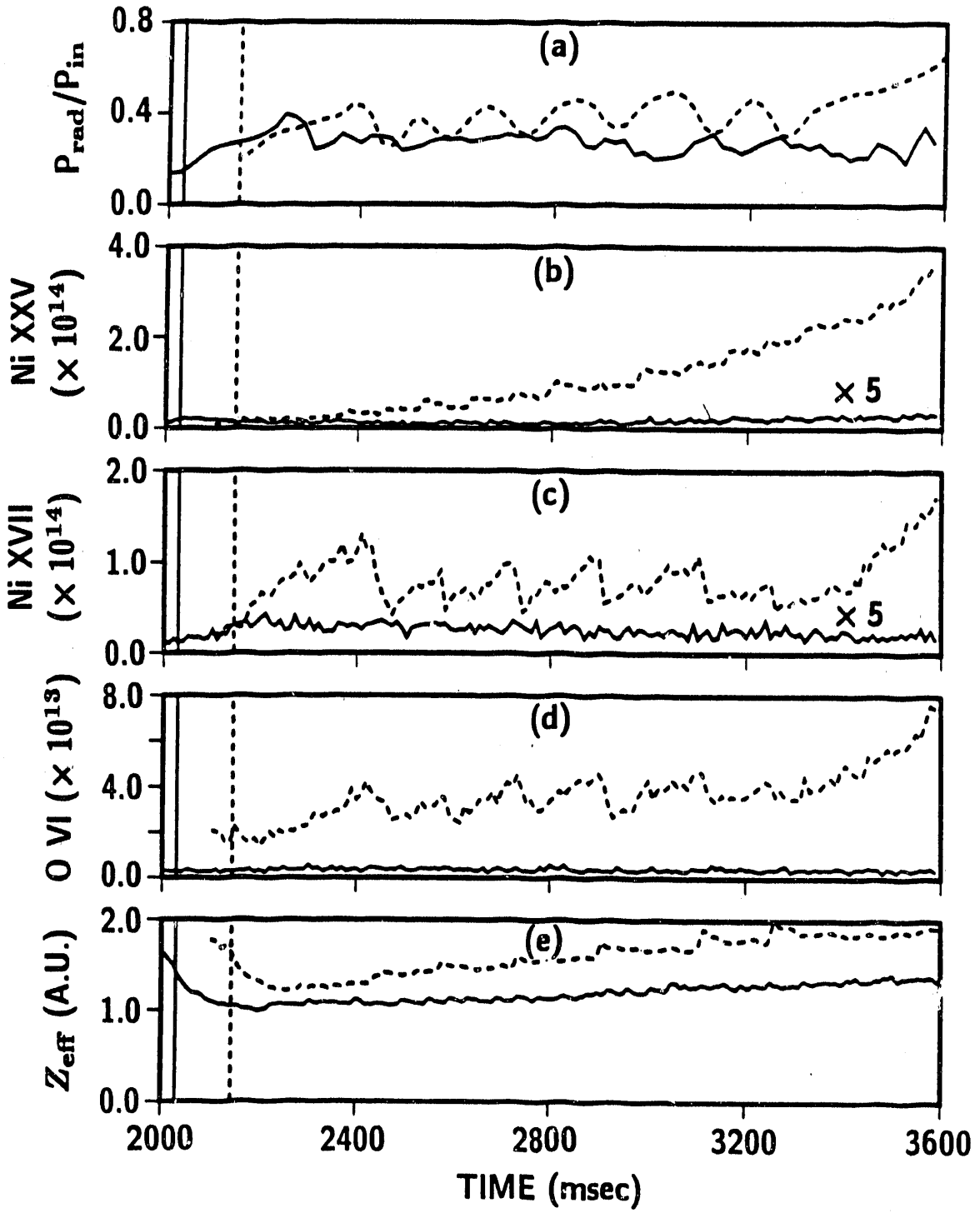

Fig. 2. After carbonization, nickel and oxygen impurity line radiation are reduced when compared to similar tokamak discharges (2.0 MA, 2.1 T, and 6.5 MW of neutral beam power) before carbonization (dashed lines). The nickel impurity lines after carbonization are multiplied by a factor of 5 in this figure. Z_{eff} and radiated power are also lower (from Ref. 8).

to boronize DIII–D was installed. Boronization is similar to carbonization in that a thin film is deposited during a glow discharge.[10] Instead of methane, diborane gas, B_2D_6, is used. The details of the DIII–D boronization process are described in an accompanying paper.[11] As shown in Fig. 3, oxygen and radiated power are further reduced below the levels produced by carbonization for comparable 2.0 MA plasma discharges. The application of boron films has allowed routine operation at up to 3 MA, and this current limit was due to the maximum ratings of the field shaping power supplies, not plasma-wall interactions. Even for 3 MA discharges, the fraction of radiated power, $P_{\rm rad}/P_{\rm auxiliary}$ is usually below 50%.

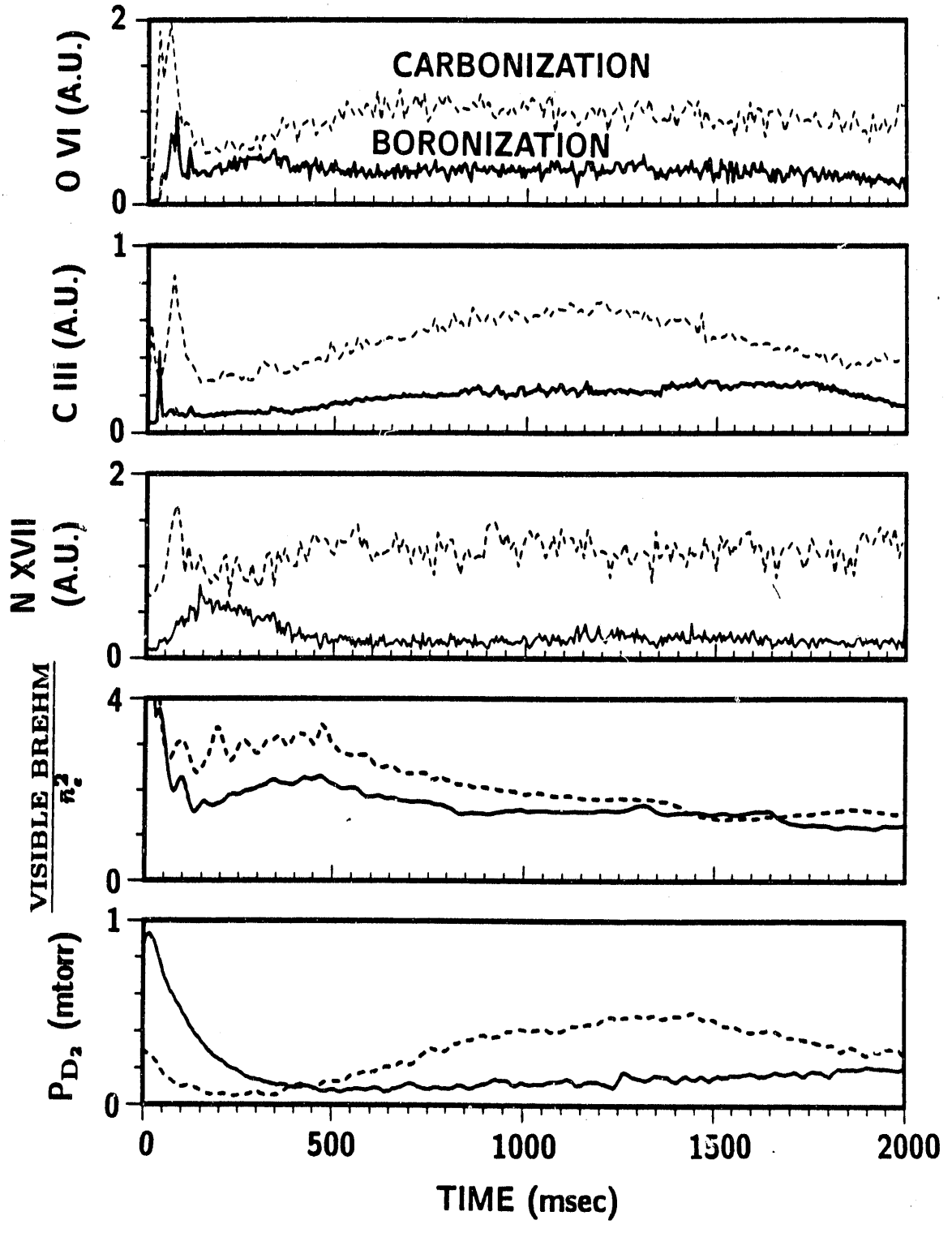

Fig. 3. Oxygen, carbon, and nickel impurity line radiation is reduced for similar discharges after boronization (solid lines) when compared to past carbonization discharges (dashed lines) (2 MA, 2.1 T, double-null divertor). Neutral pressure and Z_{eff} are also lower. The ohmic phase of the discharge is shown.

III. WALL CONDITIONING FOR RECYCLING CONTROL

A necessary condition for obtaining high confinement or high power beam heated plasmas without frequent disruptions is low impurity influx and techniques to reduce impurities in DIII–D were presented in Section II. However control of the deuterium influx is equally important and much of the recent DIII–D work in wall conditioning has been directed at reducing the hydrogenic particle fueling. The importance of reducing the hydrogenic particle influx is illustrated in Fig. 4. High neutral pressure can cause a loss of H–mode confinement, and can prohibit the attainment of H–mode altogether. An example of a failure to obtain H–mode discharges occurred after the installation of large area graphite coverage which increased the fraction of plasma facing graphite surface from 9% to 40%. The increased graphite surface was a source of hydrogenic particles so that even after recovery from the machine opening was accomplished, H–mode could not be obtained. After HeGWC was initiated before every discharge, wall fueling was reduced and H–mode discharges were again obtained.[12] Another example of the importance of low neutral pressure is the recent achievement of a regime of very high confinement (VH–mode) which was achieved after boronization. This regime has only been achieved with a low ohmic target density and low edge neutral pressure.[13]

Reduced hydrogenic particle fueling has been obtained in several ways in DIII–D: baking, HeGWC, neon glow, carbonization, and boronization. The efficacy of these techniques will be discussed below.

Baking to a high temperature (300–400°C) has successfully reduced recycling and edge neutral pressure by up to a factor of 10 and produced modest increases in H–mode confinement times of ~10%–15%.[12] However a baking session requires more than 11 hours, because the vessel must be cooled to <50°C before tokamak operations

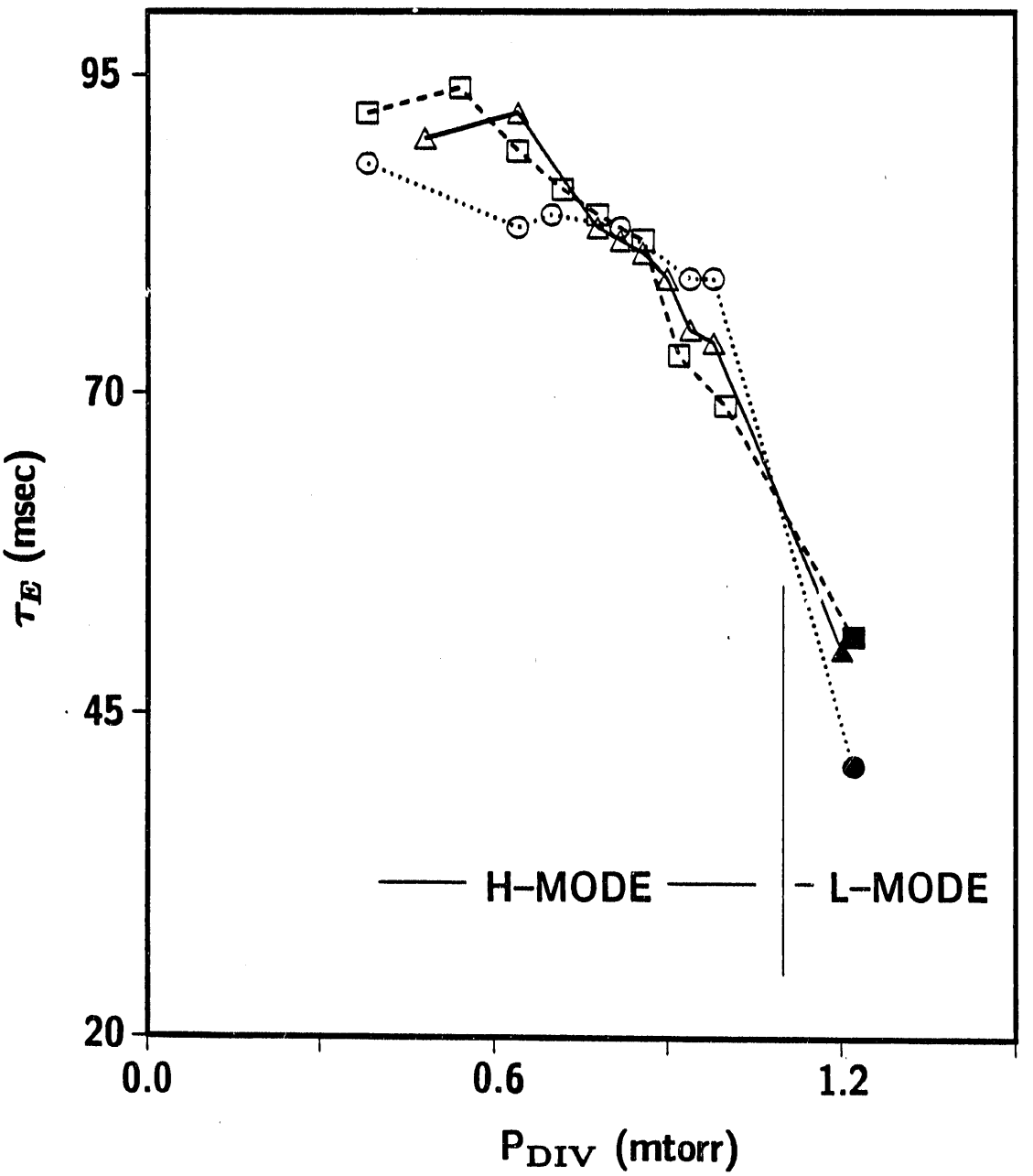

Fig. 4. Global energy confinement, τ_E, decreases as neutral pressure in the divertor region increases. Above 1 mTorr the tokamak discharge returns to L–mode confinement (1.25 MA, single-null divertor, 2.1 T, from Ref. 12).

can commence. Although recycling is initially low, it increases every discharge as the graphite becomes saturated. With 9% graphite coverage, neutral pressure and D_α line radiation increased with a 5 to 7 discharge e-fold after baking.[12]

Repetitive HeGWC between tokamak discharges is also effective in reducing wall fueling. A helium glow discharge desorbs deuterium from the surface and near surface layers of graphite. Since the saturated helium concentration in graphite is much lower than deuterium in graphite, helium fueling of a tokamak discharge after a session of HeGWC is not a problem. The effectiveness of HeGWC is illustrated in Fig 5 where the helium glow was not used for four discharges. Both the D_α intensity and the divertor neutral pressure increase dramatically from the first to the fourth discharge without HeGWC. Because the effects of HeGWC are transient, as shown in Fig. 5, this technique is used before every discharge.[4]

Neon (and argon) glow discharges between tokamak shots have also been utilized to reduce hydrogenic fueling. Since these inert gases have a higher mass than helium, they might be more effective in desorbing D_2 from the graphite surface and lower recycling even more than HeGWC. Two comparison discharges, one preceded by neon glow and another preceded by helium glow are shown in Fig. 6 for an inside wall limited discharge. While neon glow did lower the deuterium recycling inferred from the D_α line intensity, enough neon was retained in the graphite and released during the tokamak discharge to increase $Z_{\rm eff}$ and radiated power. It is possible that neon glow, followed by helium glow to desorb the neon might be effective in achieving lower recycling and wall particle fueling with low values of $Z_{\rm eff}$ and radiated power, but this has not yet been attempted in DIII–D.

Carbonization has also been used to reduce recycling. After the first carbonization of DIII–D, accompanied by a post carbonization bake to 350°C, divertor D_α emission was initially reduced by a factor of 5 to 10.[8] However, this effect only lasted one experimental day (~30 discharges). The combination of baking and an increased surface area to act as a reservoir for deuterium was the probable cause of the lower

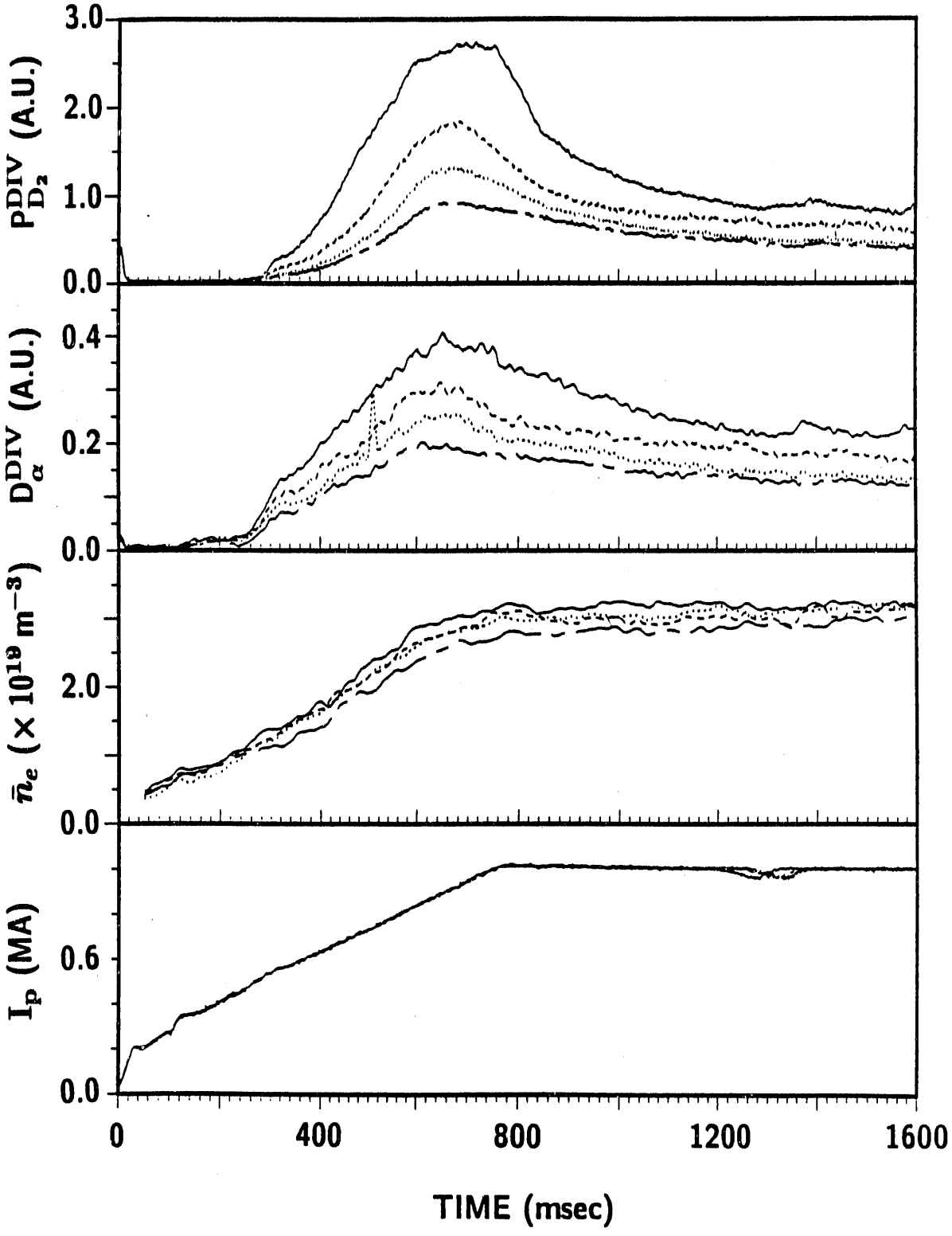

Fig. 5. Neutral pressure and D_α line radiation increase every discharge after repetitive HeGWC is terminated. After four discharges, both have increased by approximately a factor of two.

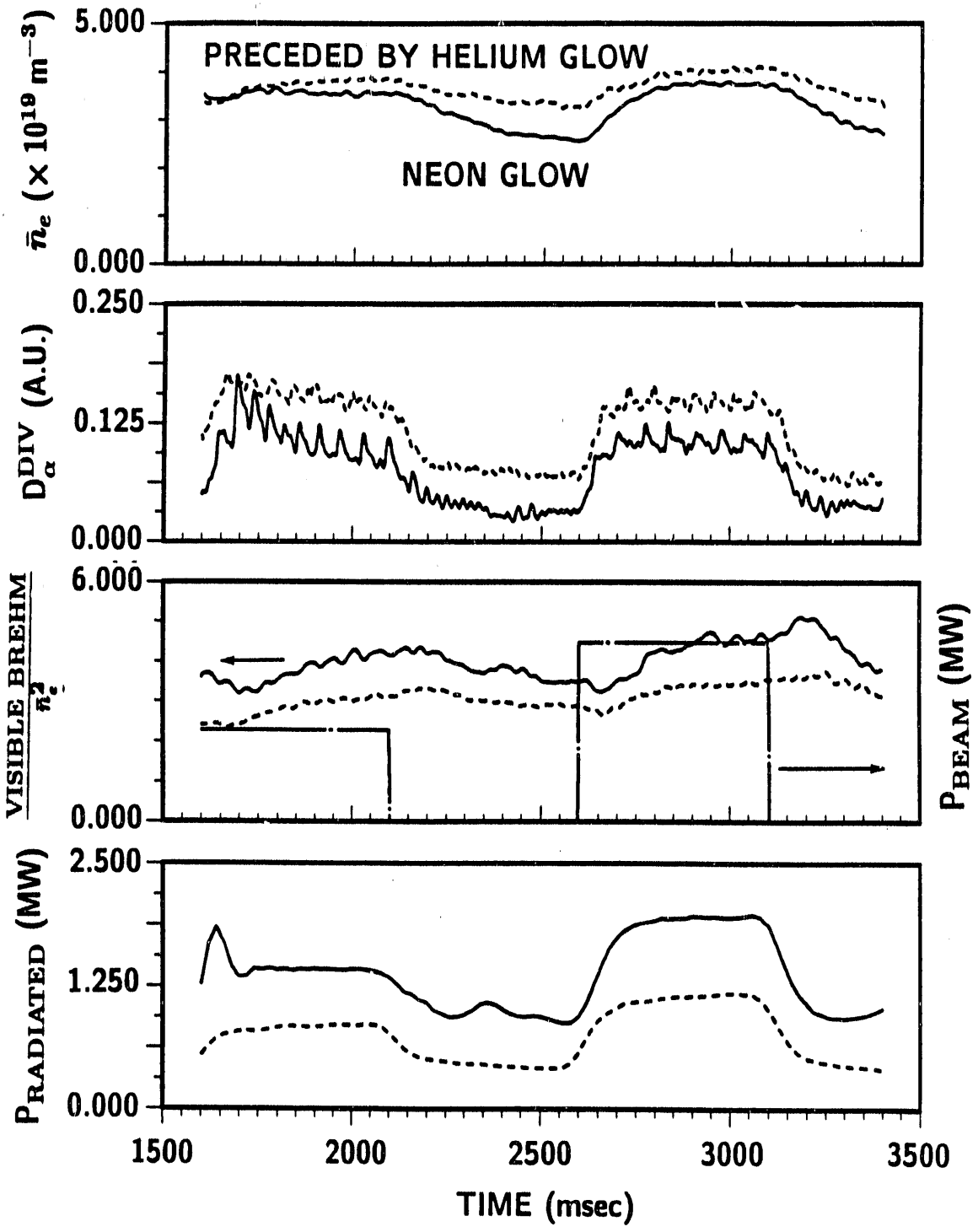

Fig. 6. Deuterium recycling is reduced on a subsequent discharge after a session of neon glow (solid lines) when compared with a similar discharge preceded by helium glow (dashed lines). However Z_{eff}, which is proportional to visible bremsstrahlung/$\bar{n}_e^2$, and radiated power both increase after a session of neon glow, which limit the effectiveness of this wall conditioning technique.

recycling. Although the effect of reduced recycling after carbonization and baking lasted longer than baking only, it was still transient. The carbonization discharges shown in Fig. 7 are more than 150 discharges after the initial carbonization and the low recycling condition has been lost. In this case, the larger reservoir of both saturated carbon tiles and the carbon film produced a higher hydrogenic fueling rate than without carbonization. This further illustrates the importance of baking in reducing recycling.

As discussed in the last section, boronization has recently been implemented to further reduce impurities. It has also had the additional benefit of reducing the initial rate of density rise after the L–mode to H–mode transition, shown in Fig. 7. One characteristic of DIII–D H–mode discharges without edge localized modes (ELMs) is an uncontrolled density rise. This has proved to be the most difficult phase of the discharge to control, since the particle confinement time, τ_p, and the fueling efficiency increase dramatically during H–mode. After boronization there was a significant reduction in τ_p^*, defined as $\tau_p^* = \tau_p/(1-R)$, where τ_p is the particle confinement time and R is the recycling coefficient. τ_p^* is shown in Figs. 8 and 9 for four phases of a post-boronization discharge. Note that different phases of the discharge can have different particle confinement times (and possibly different values of R). τ_p^* is measured by the exponential increase or decrease of the electron density after a change in either the beam fueling, or a change in the particle confinement time, *i.e.* going from L–mode to H–mode. We assume in this analysis that $N_D \sim N_e = \bar{n}_e V_p$ (*i.e.* $Z_{eff} = 1$) and thus τ_p^* can be determined from a least squares fit of the average electron density. Plasma volume, V_p, is calculated from an MHD equilibrium fit to magnetic probe data. Before boronization, these density fits were difficult to obtain, presumably because Γ_{wall} and R are time dependent. However, as shown in Fig. 8, very good agreement is obtained for post-boronization discharges.

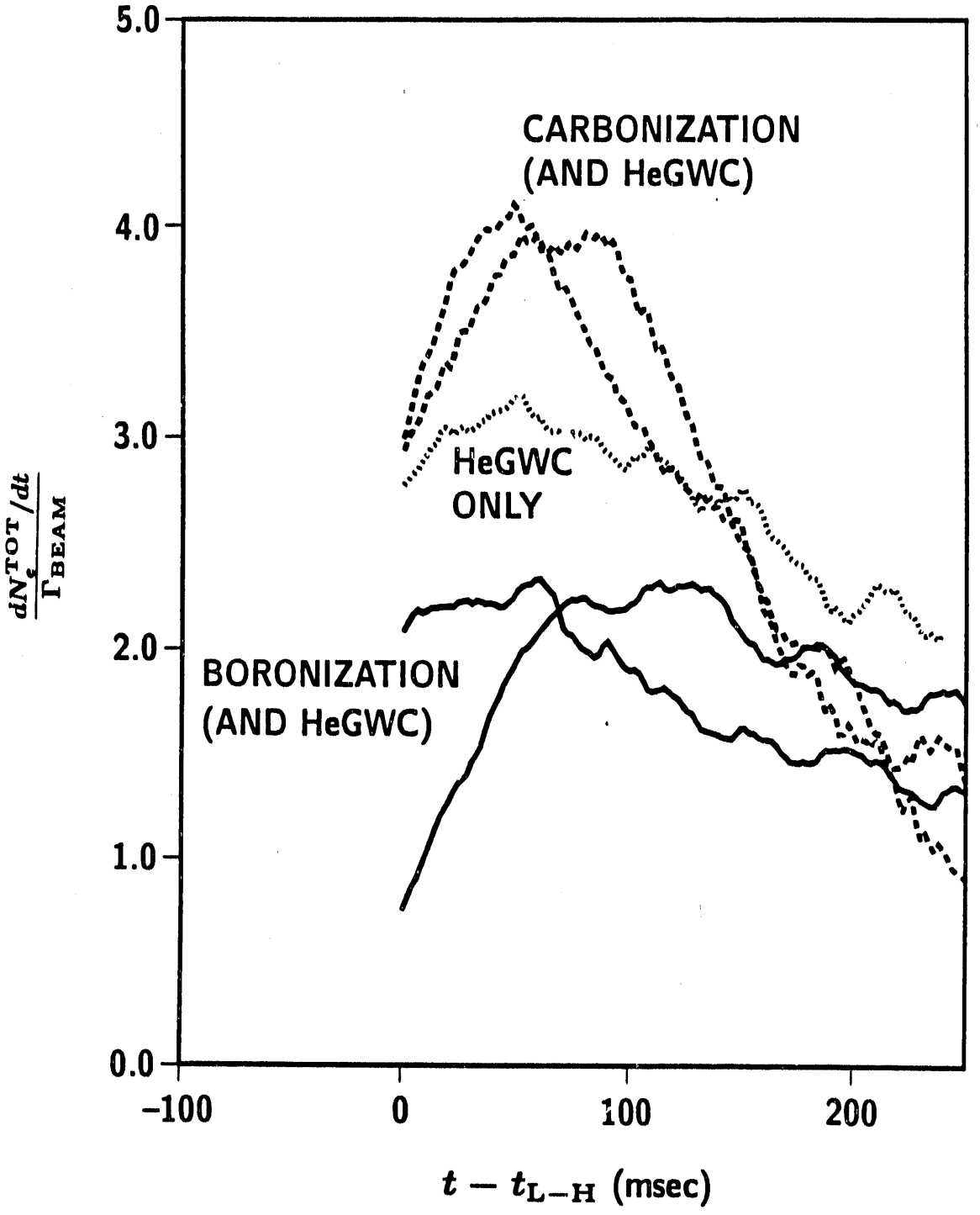

Fig. 7. The initial rate of rise total electrons, dN_e/dt, normalized to the particle fueling from neutral beam injection, Γ_{beam}, is lower for tokamak discharges after boronization (solid line) than for discharges after carbonization (dashed line) or HeGWC (dotted line). Discharge parameters: 2.0 MA, 2.1 T, double-null divertor. The first 250 msec of the ELM-free phase is shown.

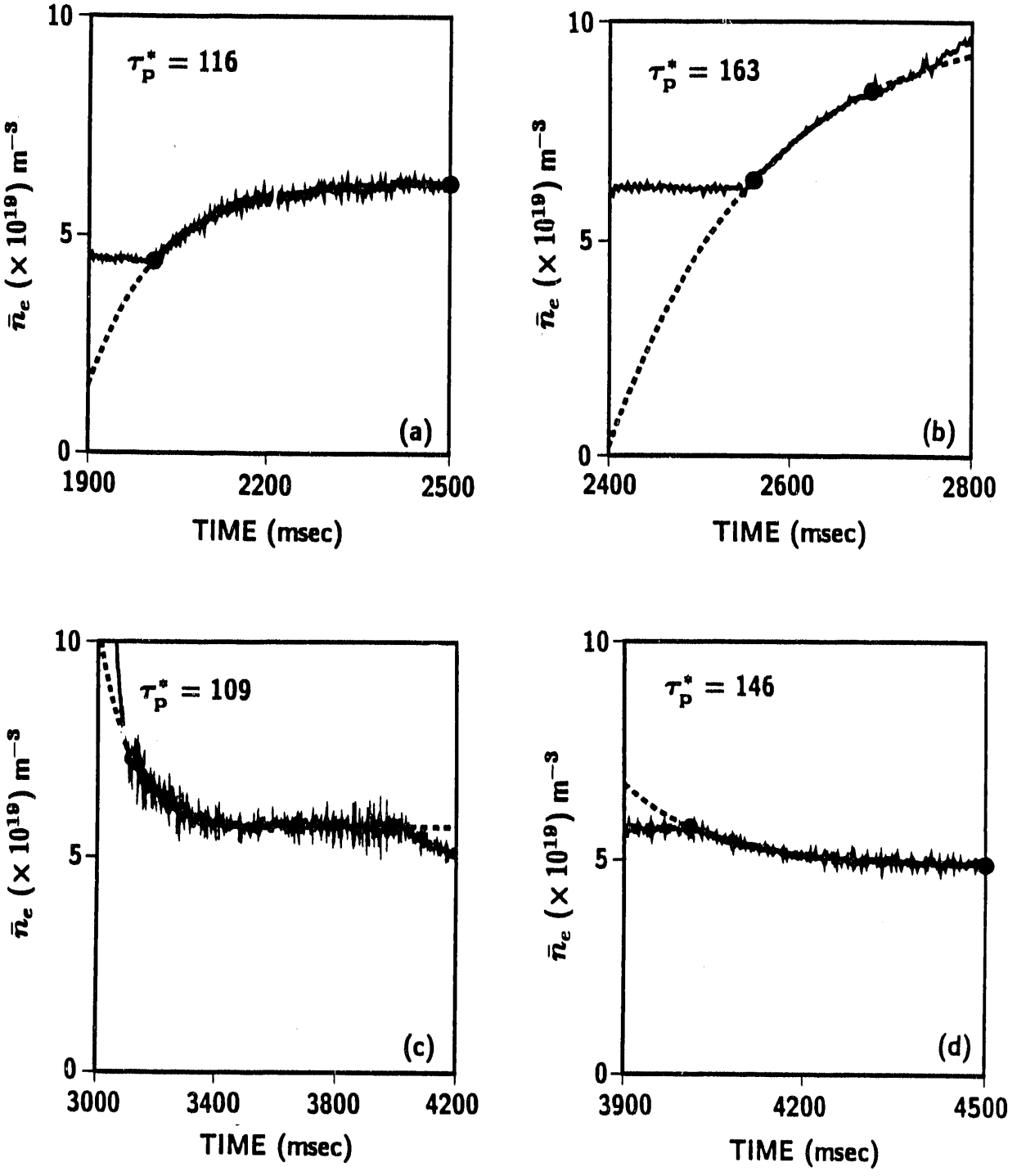

Fig. 8. The density decay constant, τ_p^*, is calculated by a fit to the exponential rise or decay of electron density, Eq. (1), for four different phases of a post-boronization discharge: (a) L–mode, 12.3 MW, (b) VH–mode, 12.3 MW, (c) L–mode, 2.8 MW, and (d) the ohmic phase. The least squares fit is shown as a dashed line and the range over which the fitting was done is defined by solid circles.

The temporal evolution of this discharge is shown in Fig. 9. There is a 500 ms long L–mode phase after the application of neutral beam power, followed by an ELM-free phase and then ELMing H–mode. In this discharge, a reduction in beam heating power causes a transition from H–mode back to L–mode approximately 50 ms later; so this more complicated behavior was not fit. It is possible to obtain values of τ_p^* for four phases of the discharge and these are shown in Fig. 8, along with the global energy confinement times in these phases of the discharge.

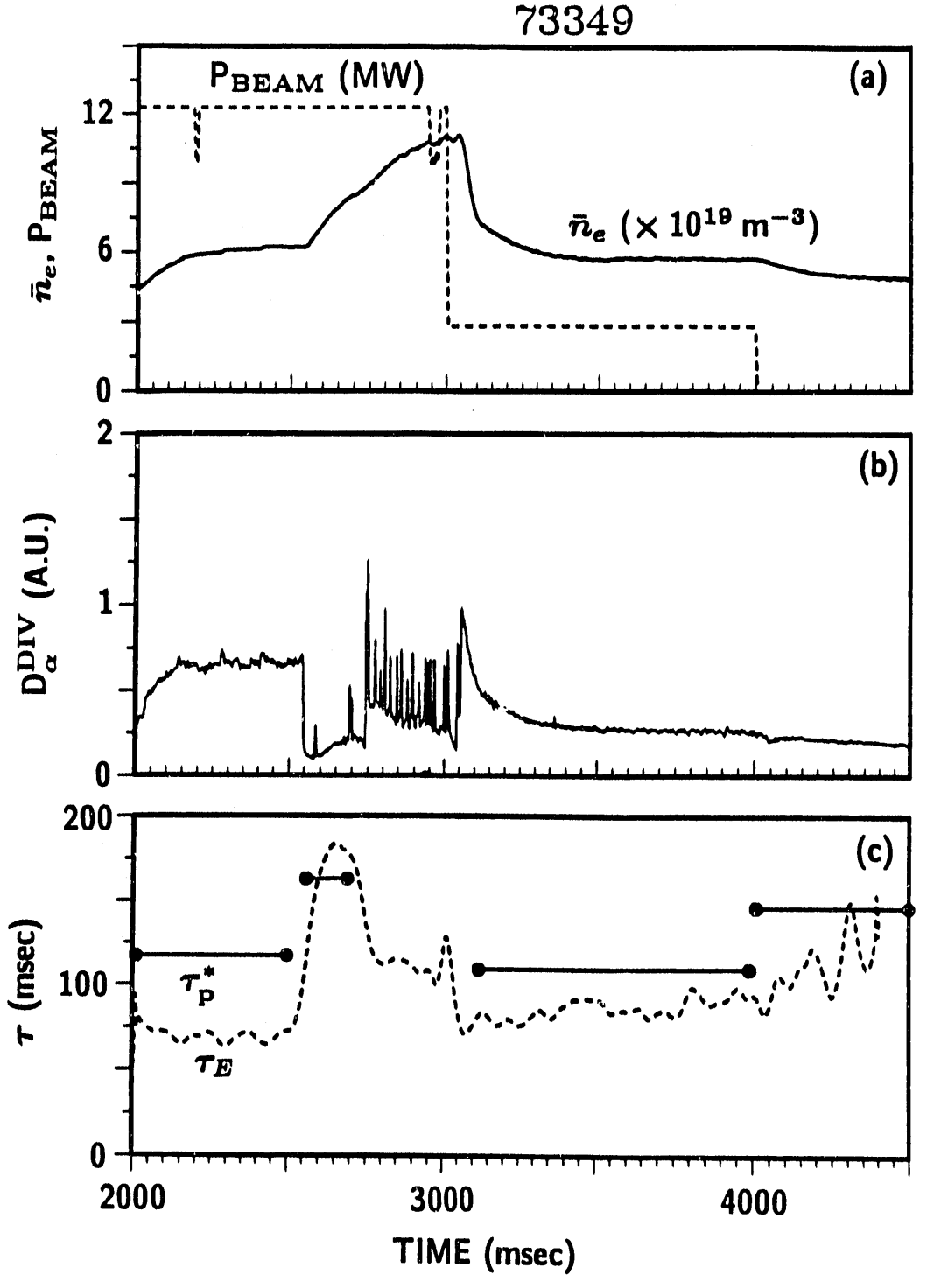

Fig. 9. Electron density, D_α, τ_E, and τ_p^* as a function of time. (c) The values of τ_p^* are shown (solid line) for four phases of the discharge and the regions over which τ_p^* was fit are delineated by closed circles. Global energy confinement time, τ_E, is also shown for comparison (dashed line). The exponential fits which determine τ_p^* are displayed in Fig. 8.

IV. DISCUSSION

Boronization has produced the lowest values of recycling and the lowest values of impurities of all techniques used in DIII–D to date to reduce particle fueling and impurities. After boronization a new confinement regime, VH–mode, has been observed characterized by energy confinement from 1.5 to 2 times the previous DIII–D-JET H–mode confinement scaling relation and a factor of up to 3.5 times the ITER-89P L–mode scaling.[13] Necessary conditions to achieve VH–mode are low target density, low neutral pressure, a low fraction of radiated power, $P_{\rm rad}/P_{\rm nb} \leq 0.25$ during L–mode and $P_{\rm rad}/P_{\rm nb} \leq 0.50$ during the the VH–mode phase of the discharge. To date, boronization is the only wall conditioning technique which has produced the conditions necessary to achieve VH–mode. As shown in Fig. 8 and Fig. 9, $\tau_{\rm p}^*$ is very low in these discharges, <170 ms in all phases shown. For comparison, $\tau_{\rm p}^* \sim 0.5$–1 sec for similar discharges preceded by HeGWC only. $\tau_{\rm p}$ is difficult to determine in diverted discharges and no measurement of $\tau_{\rm p}$ has been made after boronization. However, it is clear that the recycling coefficient, R, is less than unity. The comparison shown in Fig. 7 also indicates that either R or wall fueling (or both) is lower after boronization.

A model to describe these observations is discussed below. Wall fueling is a significant contribution to this particle balance equation. The discharge shown in Fig. 8 and Fig. 9 is a double-null diverted discharge and there is a large heat and particle flux near the intersection of the separatrix with the wall. We assume that this wall interaction is the dominant particle source, and since this wall interaction is accompanied by erosion of the deuterium rich boron film, this could represent the source of particles, $\Gamma_{\rm wall}$. On other parts of the wall, the helium glow discharge preceding the tokamak discharge has desorbed deuterons allowing these parts of the

wall, not exposed to direct plasma-wall interaction, to act as a sink, *i.e.* they can pump any incident particles.

With the assumptions discussed above, the particle balance can be described by:

$$\frac{dN_{\rm D}}{dt} = \Gamma_{\rm beam} + \Gamma_{\rm beam}^{\rm gas} + \Gamma_{\rm fuel} + \Gamma_{\rm wall} - N_{\rm D}/\tau_{\rm p}^{*} \quad , \tag{1}$$

where $\Gamma_{\rm beam}^{\rm gas}$ is the flux of neutral gas, D_2, from the neutral beam ducts; $\Gamma_{\rm fuel}$ is the external D_2 gas fueling; $N_{\rm D} = \bar{n}_{\rm e} V_{\rm p}$ is the total number of deuterons in the plasma discharge, assuming $Z_{\rm eff} = 1$. During neutral beam injection, $\Gamma_{\rm fuel}$ is zero and the contribution of $\Gamma_{\rm beam}^{\rm gas}$ can be neglected. Thus the solution to Eq. (1) is

$$N_{\rm D} = (\Gamma_{\rm beam} + \Gamma_{\rm wall})\ \tau_{\rm p}^{*} + \left[N_{D0} - (\Gamma_{\rm beam} + \Gamma_{\rm wall})\ \tau_{\rm p}^{*}\right]\ e^{-(t-t')/\tau_{\rm p}^{*}} \quad . \tag{2}$$

In this equation, N_{D0} is the initial number of deuterons present at time t', when there is an abrupt change in either the neutral beam fueling (a change in beam power) or the particle confinement (a transition from L–mode to H–mode). Note that there are four such times shown in Fig. 8, so $\tau_{\rm p}^{*}$ in four phases of the discharge can be determined. (We have not determined a value of $\tau_{\rm p}^{*}$ for ELMing H–mode or for the transition from H–mode back to L–mode since this transition was immediately preceded by a reduction in the neutral beam power.) A least squares fit to the electron density, as shown in Fig. 8, has the form

$$\bar{n}_{e} = \frac{N_{\rm D}}{V_{\rm p}} = a + b\, e^{-(t-t')/\tau_{\rm p}^{*}} \quad . \tag{3}$$

Since Γ_{beam} is known, Γ_{wall} can be determined from Eqns (2) and (3). Table II summarizes the particle fueling from the wall for the four discharge phases shown in Figs. 8 and 9. The wall fueling is the dominant source of particles in all phases. Furthermore there is only a modest increase in Γ_{wall} from the ohmic phase [Fig. 8(d)] to the beam-heated phases which were examined. In this model we have assumed that different parts of the wall can simultaneously act as a particle source (Γ_{wall}) and as a sink for particles flowing out of the plasma [$N_{Do}/\tau_p^* = (1-R)\frac{N_{Do}}{\tau_p}$.]

Table II
Wall Fueling Calculated from Exponential Fits to the Electron Density for Four-Phases of the Discharge in Fig. 9

Transition or Change in Beam Power	Time Range of τ_p^* FIT During Discharge	τ_p^* (ms)	Γ_{beam} (atoms/s)	Γ_{wall} (atoms/s)
P_{beam} 3.4 MW to 12.3 MW (L-mode)	2010–2500	117	1.5×10^{21}	10.3×10^{21}
L-mode to H-mode (no ELMs)	2560–2690	163	1.5×10^{21}	12.1×10^{21}
P_{beam} 12.3 MW to 3.1 MW (L-mode)	3120-3990	109	0.38×10^{21}	1.11×10^{21}
L-mode $\rightarrow$ ohmic	4010–4500	146	0	7.4×10^{21}

In conclusion, a variety of techniques have been successfully applied on DIII–D to reduce both particle and impurity influxes. The application of these techniques have produced a significant enhancement in the parameter range over which DIII–D operates. The most effective technique used so far is boronization. After the application of

a boron film we have obtained a new regime of very high confinement, VH–mode. With VH–mode, a record triple product in DIII–D, $N_D(0)\tau_E\, T_i(0) = 2 \times 10^{20}\,\mathrm{m}^{-3}\,\mathrm{sec\ keV}$, has been achieved. Future work on first wall materials and preparation will emphasize both impurity reduction and particle fueling. We are investigating boronization before each tokamak discharge to reduce recycling and plan to install a cryopump to actively pump D_2 during tokamak discharges.

ACKNOWLEDGMENT

This work was supported by the U.S. Department of Energy under Contract No. DE-AC03-89ER51114.

REFERENCES

[1] L. Oren and R.J. Taylor, Nucl. Fusion **17**, 1143 (1977).

[2] G. M. McCracken and P. E. Stott, Nucl. Fusion **19**, 889 (1979).

[3] J. D. Strachan, M. Bitter, A. T. Ramsey, et al., Phys. Rev. Lett. **58**, 1004 (1987).

[4] G. L. Jackson, T. S. Taylor, and P. L. Taylor, Nucl. Fusion **30**, 2305 (1990).

[5] G. L. Jackson, R. E. Clausing, A. F. Lietzke, et al., J. Vac. Sci. Technol. **A1**, 1861 (1983).

[6] N. H. Brooks, P. Petersen, and The DIII–D Group, J. Nucl. Mater. **145-147**, 770 (1987).

[7] K. H. Burrell, S. Ejima, D. P. Schissel, et al., Phys. Rev. Lett. **59**, 1432 (1987).

[8] G. L. Jackson, J. Winter, S. Lippmann, et al., J. Nucl. Mater. **185**, 139 (1991).

[9] R. D. Stambaugh and The DIII–D Team, in *Proc. 13th Intnl Conf. on Plasma Physics and Contr. Nucl. Fusion*, (IAEA-CN-53/A-I-4, 1991) Vol. 1, p. 69.

[10] J. Winter, J. Nucl. Mater. **176-177**, 14 (1990).

[11] J. Phillips, T. Hodapp, K. Holtrop, et al., General Atomics Report GA-A20750 (1991), and to be published in these proceedings.

[12] G. L. Jackson, T. S. Taylor, S. L. Allen, J. Nucl. Mater. **162-164**, 489 (1989).

[13] G. L. Jackson, and the DIII–D Team, "Very High Confinement Discharges in DIII–D After Boronization," to be presented at 33rd Annual Meeting of the American Physical Society, Division of Plasma Physics, November 4–8, 1991 in Tampa, Florida and published in a special issue of Phys. Fluids B.

END

DATE FILMED

3 / 16 / 92